A Novel Persistent Tetrodotoxin-Resistant Sodium Current In SNS-Null And Wild-Type Small Primary Sensory Neurons

Theodore R. Cummins,[1,2] Sulayman D. Dib-Hajj,[1,2] Joel A. Black,[1,2] Armen N. Akopian,[3] John N. Wood,[3] and Stephen G. Waxman[1,2]

[1]Department of Neurology and PVA/EPVA Neuroscience Research Center, Yale Medical School, New Haven, Connecticut 06510, [2]Rehabilitation Research Center, Veterans Administration Connecticut Healthcare Center, West Haven, Connecticut 06516, and [3]Department of Biology, University College London, London WC1E 6BT, United Kingdom

TTX-resistant (TTX-R) sodium currents are preferentially expressed in small C-type dorsal root ganglion (DRG) neurons, which include nociceptive neurons. Two mRNAs that are predicted to encode TTX-R sodium channels, SNS and NaN, are preferentially expressed in C-type DRG cells. To determine whether there are multiple TTX-R currents in these cells, we used patch-clamp recordings to study sodium currents in SNS-null mice and found a novel persistent voltage-dependent sodium current in small DRG neurons of both SNS-null and wild-type mice. Like SNS currents, this current is highly resistant to TTX (K_i = 39 ± 9 μM). In contrast to SNS currents, the threshold for activation of this current is near −70 mV, the midpoint of steady-state inactivation is −44 ± 1 mV, and the time constant for inactivation is 43 ± 4 msec at −20 mV. The presence of this current in SNS-null and wild-type mice demonstrates that a distinct sodium channel isoform, which we suggest to be NaN, underlies this persistent TTX-R current. Importantly, the hyperpolarized voltage-dependence of this current, the substantial overlap of its activation and steady-state inactivation curves and its persistent nature suggest that this current is active near resting potential, where it may play an important role in regulating excitability of primary sensory neurons.

Key words: sodium current; persistent current; dorsal root ganglion; excitability; tetrodotoxin; sensory neuron

Small dorsal root ganglion (DRG) neurons (which include nociceptive cells) are unusual in expressing tetrodotoxin-resistant (TTX-R) sodium currents, in addition to the TTX-sensitive (TTX-S) sodium currents that are present in many neurons (Kostyuk et al., 1981). Because of their preferential expression in nociceptive neurons, the channels responsible for these TTX-R currents are of special interest. One TTX-R channel that has been cloned from DRG neurons, SNS (Akopian et al., 1996; Sangameswaran et al., 1996), produces a slowly inactivating sodium current ($\tau_{inactivation}$, ~5 msec for the peak current) with relatively depolarized voltage dependence of activation and inactivation. A second sodium channel, NaN, with a sequence predicting a TTX resistance similar to that of SNS, is also preferentially expressed in small DRG neurons (Dib-Hajj et al., 1998, 1999; Tate et al., 1998).

A recent study on DRG neurons from SNS-null mutant mice demonstrated only TTX-S sodium currents (Akopian et al., 1999). These findings were unexpected in light of the presence of NaN transcript within these cells. The present study revisits this issue and shows that DRG neurons from SNS-null mice (Akopian et al., 1999) express a TTX-R sodium current with novel properties. We also demonstrate that this TTX-R current is present in small wild-type (WT) mouse DRG neurons. The relatively hyperpolarized voltage dependence of activation and inactivation of this current and its persistent nature suggest that it contributes to setting the firing properties of small DRG neurons by modulating their resting potentials and/or thresholds.

MATERIALS AND METHODS

Whole-cell patch-clamp recordings. DRG cultures from L4 and L5 ganglia of WT and SNS-null mice (Akopian et al., 1999) were established as previously described (Cummins and Waxman, 1997). Sodium currents were studied in small (18- to 27-μm-diameter) DRG neurons after short-term culture (6–24 hr); at this time in culture, neurites are not generally present. Whole-cell patch-clamp recordings were conducted at room temperature (~21°C) using an EPC-9 amplifier and the Pulse program (version 7.89). Fire-polished electrodes (0.8–1.5 MΩ) were fabricated from 1.7 mm capillary glass using a Sutter P-97 puller. The average cell capacitance was 21 ± 1 pF (mean ± SE; n = 55) for WT and 23 ± 1 pF (n = 91) for SNS-null cells. The average access resistance was 2.1 ± 0.1 MΩ for WT and 2.0 ± 0.1 MΩ for SNS-null cells. Voltage errors were minimized using 80% series resistance compensation. The maximum theoretical voltage error was 2 ± 1 mV for TTX-R sodium currents in SNS-null neurons; this and the spherical nature of the cells provided

Received Sept. 3, 1999; revised Oct. 6, 1999; accepted Oct. 8, 1999.

This work was supported in part by grants from the National Multiple Sclerosis Society, the Medical Research Service and Rehabilitation Research Service, Department of Veterans Affairs (S.G.W.), and the Wellcome Trust and Medical Research Council (J.N.W. and A.N.A.).

Correspondence should be addressed to Dr. Stephen G. Waxman, Yale University School of Medicine, Department of Neurology, 707 LCI, 333 Cedar Street, New Haven, CT 06510. E-mail: Stephen.Waxman@Yale.Edu

This article is published in *The Journal of Neuroscience*, Rapid Communications Section, which publishes brief, peer-reviewed papers online, not in print. Rapid Communications are posted online approximately one month earlier than they would appear if printed. They are listed in the Table of Contents of the next open issue of JNeurosci. Cite this article as: JNeurosci, 1999, 19:RC43 (1–6). The publication date is the date of posting online at www.jneurosci.org.

http://www.jneurosci.org/cgi/content/full/3758

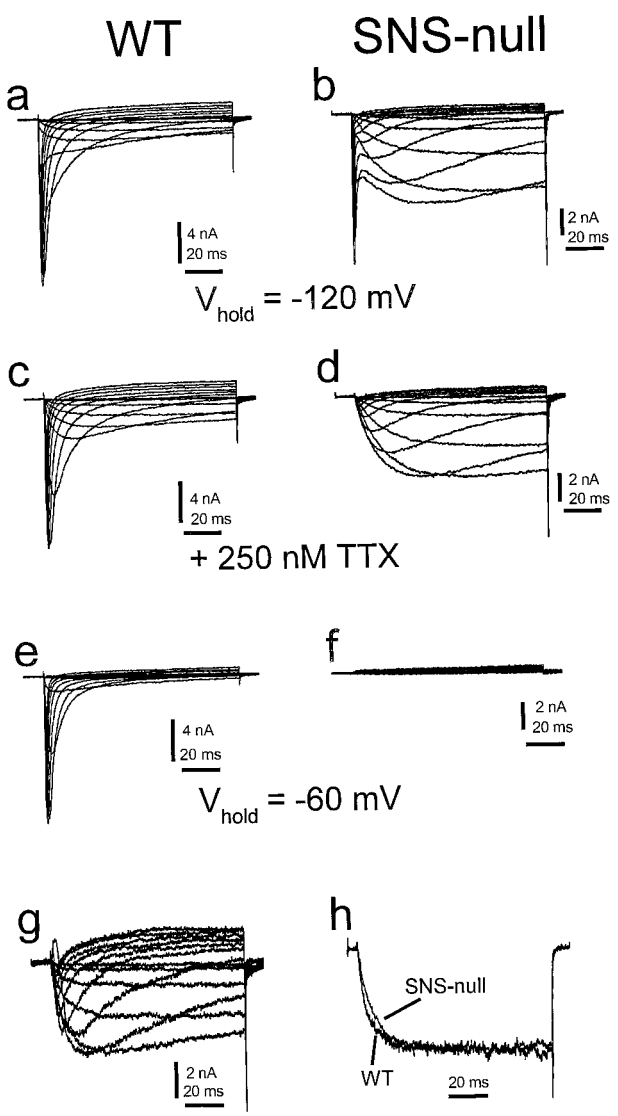

Figure 1. Multiple sodium currents are expressed in small DRG neurons from WT and SNS-null mice. *a, b*, Representative recordings from a holding potential of −120 mV. Calcium currents were blocked with 100 μM cadmium in the bath solution. *c, d*, TTX (250 nM) blocks the fast-inactivating component. A persistent current is expressed in both the WT (*c*) and SNS-null (*d*) neurons, but the slowly inactivating component is seen only in the WT neuron. *e, f*, When the neurons were held at −60 mV and a 100 msec step to −120 mV preceded the test pulses, the persistent current is not obvious in either WT (*e*) or SNS-null (*f*) neurons. *g*, Subtraction of the slowly inactivating component (*e*) from the total TTX-R current (*c*) reveals the persistent current in WT neurons. *h*, The persistent current derived by this subtraction process from WT neurons is similar to that recorded in SNS-null neurons. Test potential is −60 mV, and traces are normalized for comparison.

nearly ideal recording conditions. Linear leak subtraction was used for all recordings. The pipette solution contained (in mM): 140 CsF, 1 EGTA, 10 NaCl, and 10 HEPES, pH 7.3. The standard bathing solution was (in mM) 140 NaCl, 3 KCl, 1 $MgCl_2$, 1 $CaCl_2$, 0.1 $CdCl_2$,and 10 HEPES, pH 7.3. Cadmium was included to block calcium currents. The osmolarity of all solutions was adjusted to 310 mOsm.

RT-PCR. Total cellular RNA was extracted from trigeminal ganglia of each animal whose DRG neurons were studied to confirm the SNS-null genotype and the presence of the expected NaN products (see Fig. 3). First-strand cDNA synthesis and PCR were performed as previously described (Dib-Hajj et al., 1998).

RESULTS

Whole-cell patch-clamp recordings demonstrate the presence of fast and slow inactivating voltage-dependent inward currents from the cultured DRG neurons of WT and SNS-null mice with a holding potential of −120 mV (Fig. 1). In the presence of 250 nM TTX in the bathing solution, TTX-R inward currents were recorded from 77% of small WT neurons (24 of 31) and 74% of SNS-null neurons (37 of 50). However, the inward currents were strikingly different in the two groups of cells. The majority of WT neurons (18 of 31) showed slowly inactivating TTX-R currents (which activated between −40 and −30 mV and resemble currents in heterologously expressed SNS channels; see Akopian et al., 1996) together with persistent TTX-R currents (which did not inactivate during the 100 msec depolarization at negative test potentials). Consistent with the conclusion that SNS encodes a slowly inactivating channel (Akopian et al., 1996; Sangameswaran et al., 1996), SNS-null neurons did not express the slowly inactivating TTX-R currents. However, a persistent TTX-R current was clearly present in these cells (Fig. 1*d*), and the amplitude was as large as 11 nA. This persistent current activated between −60 and −70 mV and peaked at approximately −20 mV (peak amplitude, 5.0 ± 0.6 nA; peak density, 235 ± 77 pA/pF; $n = 22$).

Because the persistent TTX-R current was recorded with cadmium in the bath and fluoride in the pipette solution, we suspected that it was a sodium current. Whole-cell recordings of SNS-null cells in the presence of low external calcium (10–50 μM) but high external sodium (140 mM) demonstrated large persistent inward currents in 15 of 25 cells. Increasing external calcium from 50 μM to 1 mM did not increase the size of the current (Fig. 2*a*; $n = 4$). Additionally, when the external medium contained high calcium (1 mM) but zero sodium we did not observe any inward currents activating at negative potentials ($n = 15$). We could often observe small inward currents that activated near −20 mV if cadmium was not included in the external solution, but these high-voltage-activated currents could be blocked with 50–100 μM cadmium and appear to be L-type calcium currents. However, in four of six SNS-null cells tested, the low-voltage-activated (LVA) persistent inward current was revealed in the presence of cadmium when external sodium was increased from 0 to 50 mM (Fig. 2*b*). Based on these experiments, we conclude that the LVA persistent current that we observe in SNS-null neurons is indeed a sodium current.

The LVA persistent sodium current is only marginally inhibited by 1 μM TTX (6 ± 5%; $n = 6$), and as shown in Figure 2*c*, 10 μM TTX inhibited this LVA sodium current in SNS-null neurons by ~20% (estimated K_i, 39 ± 9 μM; $n = 5$). Thus, the LVA current in DRG neurons is highly resistant to TTX, like SNS (K_i, ~60 μM) (Akopian et al., 1996) and unlike the cardiac TTX-R isoform (K_i, ~1–2 μM; Satin et al., 1992).

Although the TTX resistance of the current in SNS-null DRG neurons is similar to that reported for SNS, its voltage dependence and kinetic properties are quite distinct. As seen in Figure 1*d*, the TTX-R currents in SNS-null neurons had extremely slow kinetics, with $\tau_{inactivation}$ = 43 ± 4 msec at −20 mV ($n = 18$). These currents activated at hyperpolarized potentials, with a threshold at approximately −70 mV and a midpoint of activation of −47 ± 1 mV ($n = 17$). The overshoot in the activation curve (Fig. 2*d*) could be attributable to the presence of multiple TTX-R channels in SNS-null neurons. Alternatively, it could be attributable to a TTX-R channel with complex behavior, such as one that has multiple open states or an inactivated state from which

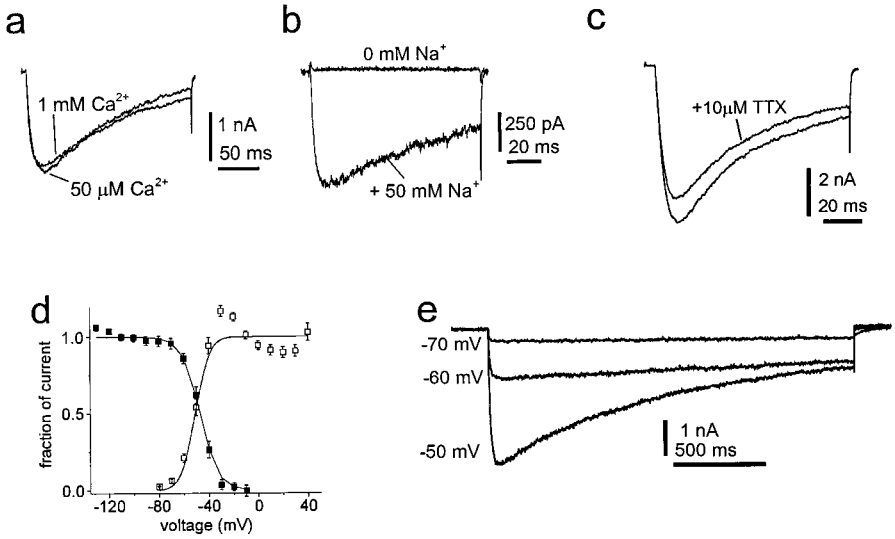

Figure 2. SNS-null neurons express a TTX-R sodium current. *a*, The current recorded from an SNS-null neuron in low calcium (50 μM) was not altered by increasing calcium to 1 mM. $V_{test} = -30$ mV. *b*, In zero sodium (160 mM TEA) inward current is not elicited by a step depolarization to −30 mV. Addition of 50 mM sodium reveals the TTX-R current. *c*, The TTX-R current in SNS-null neurons is resistant to high concentrations of TTX (10 μM). $V_{test} = -40$ mV. *d*, Activation and steady-state inactivation curves exhibit significant overlap for the TTX-R current in SNS-null neurons. The interpulse interval was 5 sec. Steady-state inactivation was measured with 500 msec prepulses. $V_{test} = -10$ mV. *e*, TTX-R persistent currents from an SNS-null neuron elicited with 2 sec step depolarizations to the voltage indicated. All recordings were made with 250 nM TTX, 100 μM cadmium, and $V_{hold} = -120$ mV.

recovery is ultraslow (ultraslow recovery from inactivation is supported by data presented below). The voltage dependence of steady-state inactivation was also fairly negative, with a midpoint of −44 ± 1 mV ($n = 10$). The considerable overlap between the activation and steady-state inactivation curves (Fig. 2*d*) should generate persistent window currents that are active near resting potential. Indeed, large persistent currents were observed in the region of overlap when the holding potential (V_{hold}) was −120 mV (Fig. 2*e*). The amplitude of the TTX-R persistent current measured at −60 mV ($V_{hold} = -120$ mV) was 1.6 ± 0.5 nA for WT neurons ($n = 17$) and 1.7 ± 0.4 nA for SNS-null neurons ($n = 22$).

Based on the midpoint of steady-state inactivation, it might be expected that large persistent TTX-R currents would also be readily observed from a V_{hold} of −60 mV; however, when the neurons were held at −60 mV and currents were elicited after a brief hyperpolarizing prepulse (100 msec at −120 mV), the persistent TTX-R current was not apparent in either WT (Fig. 1*e*) or SNS-null (Fig. 1*f*) neurons. Under these conditions, only the slowly inactivating TTX-R currents were observed in WT neurons and, as previously reported by Akopian et al. (1999), who studied cells with relatively depolarized holding potentials, there was no obvious TTX-R current in SNS-null neurons. Consistent with this, we found a prominent ultraslow inactivation of the LVA channels ($\tau_{recovery} = 16 \pm 4$ sec at −120 mV in SNS-null neurons; $n = 5$). For SNS-null neurons that expressed large TTX-R currents (peak amplitude = 8.0 ± 1.2 nA with V_{hold} of −120 mV), the peak amplitude elicited after a 100 msec prepulse to −120 mV from a V_{hold} of −60 mV was only 260 ± 57 pA ($n = 8$), indicating that ~97% of the LVA TTX-R channels are ultraslow-inactivated at −60 mV. We observed a similar ultraslow inactivation for the LVA TTX-R current in WT neurons.

Because of the ultraslow inactivation of the LVA TTX-R currents, subtraction of the slowly inactivating current recorded with $V_{hold} = -60$ mV from total TTX-R current would be expected to yield the persistent current in WT neurons. In fact, an LVA TTX-R current could be derived in this way in WT neurons (Fig. 1*g*) and closely matched the persistent current recorded in SNS-null DRG neurons (Fig. 1*h*). Thus we can isolate LVA TTX-R currents with similar properties in both WT and SNS-null DRG neurons.

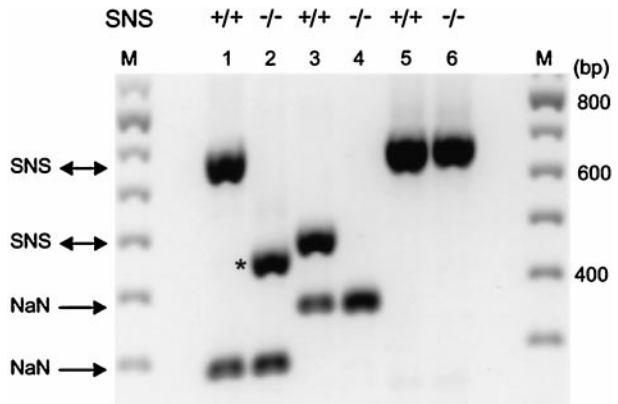

Figure 3. RT-PCR products from DRG of WT (+/+) and SNS-null (−/−) mutant mice. SNS and NaN products were co-amplified from WT (*lanes 1, 3*), and SNS-null mutants (*lanes 2, 4*). Two primer pairs, Pr1 and Pr2, for SNS were previously described (Pr1, *lanes 1, 2*; Akopian et al., 1999; Pr2, *lanes 3, 4*; F1/R2; Dib-Hajj et al., 1998). The sizes of SNS products from WT tissue using Pr1 and Pr2 are consistent with the predicted lengths of 673 bp (nucleotides 100–772) and 482 bp (nucleotides 594–1075), respectively. The smaller SNS product (denoted by an *asterisk* in *lane 2*; 450 bp) from SNS-null tissue is consistent with splicing exon 3 to exon 6 (Akopian et al., 1999), whereas lack of SNS signal in *lane 4* is attributable to the replacement of F1-containing sequence by the PGK-neo cassette in the null allele. Primers for mouse NaN amplify nucleotides 708–995 (288 bp; *lanes 1, 2*) and 626–995 (370 bp; *lanes 3, 4*) (Dib-Hajj et al., 1999). Comparable levels of glyceraldehyde-3-phosphate dehydrogenase were amplified from WT (*lane 5*) and SNS-null mutants (*lane 6*) using primers that were previously described (Dib-Hajj et al., 1998).

The molecular identity of the novel persistent TTX-R current cannot be positively determined at this time. However, transcripts for NaN, which is predicted to encode a TTX-R channel, are present in WT and SNS-null trigeminal ganglia (Fig. 3, *lanes 1–4*) and DRG neurons (data not shown). Residual SNS transcript in SNS-null ganglia lacks the sequence encoded by exons 4 and 5 (Fig. 3, *lanes 1–4*), which truncates the protein because of a reading frame shift in exon 6 (Akopian et al., 1999). Therefore, we suggest that NaN underlies this novel TTX-R persistent current.

DISCUSSION

In this study we have identified and characterized a novel persistent TTX-R sodium current in SNS-null and WT small-diameter DRG neurons. Although previous studies have suggested the presence of multiple TTX-R currents in DRG neurons, these currents have been either slowly inactivating, with time constants of 3–8 msec (Rizzo et al., 1994; Rush et al., 1998), or rapidly inactivating (time constants <2 msec; Scholz et al., 1998). TTX-R persistent currents have not been previously identified. The persistent currents that have been reported in large sensory neurons (Baker and Bostock, 1997) and other neuronal cell types, e.g., cortical (Crill, 1996) and thalamocortical neurons (Parri and Crunelli, 1998), are TTX-S. The persistent TTX-R current in small sensory neurons thus appears to be a distinct sodium current, not present in other types of neurons.

The kinetic properties of the LVA TTX-R persistent current that we describe here are different from those of SNS currents. In contrast to SNS currents, which activate at approximately −30 mV, the TTX-R persistent current activated around resting potential (approximately −70 to −60 mV). This may have important functional implications, because there are few channels of any kind that are active near resting potential, so that even small persistent currents can have a significant influence on excitability (Crill, 1996). Although the LVA persistent current in SNS-null neurons was quite large when elicited from hyperpolarized holding potentials, suggesting a relatively high density of channels, it was greatly reduced near normal resting potential (approximately −60 mV for small DRG neurons) by an apparent ultraslow inactivation. Ultraslow inactivation decreased the amplitude of the LVA TTX-R persistent current by >95% with $V_{hold} = -60$ mV and should result in a low probability of opening of any single channel around resting potential. One possible advantage is that a large number of channels with a low open probability might produce a small yet more consistent current than a smaller number of channels with a higher probability of opening.

Based on the reduced amplitude observed when the cells are held near resting potential, it is expected that the LVA TTX-R persistent current will not play a prominent role in generating action potentials. On the other hand, the properties of this current suggest that it may contribute to setting the resting potential and to the modulation of neuronal excitability close to resting potential. Persistent sodium currents have been implicated in subthreshold oscillations (Kapoor et al., 1997), in amplification of depolarizing inputs (Schwindt and Crill, 1995), and in impulse initiation (Stafstrom et al., 1982). The LVA TTX-R persistent current that we describe here might similarly be expected to have important consequences on subthreshold electrogenesis in small DRG neurons.

A previous study on SNS-null neurons (Akopian et al., 1999) did not observe the persistent TTX-R currents that we describe here. Two methodological differences may account for the failure of Akopian et al. to detect this current: (1) Akopian et al. used depolarized holding potentials, at which the LVA TTX-R persistent current is slow-inactivated and thus not detectable; and (2) Akopian et al. studied SNS-null neurons after 1–5 d in culture. Although we observed large TTX-R currents in SNS-null neurons studied after <24 hr in culture, these currents were greatly reduced in amplitude at longer times in culture (data not shown).

DRG neurons are known to express at least six sodium channel transcripts (Black et al., 1996; Dib-Hajj et al., 1998). Only two of these, SNS and NaN, are predicted to encode TTX-R currents. DRG neurons do not express mRNA for the TTX-R cardiac channel (Donahue, 1995; Black et al., 1998; Akopian et al., 1999), and SNS-null neurons do not express functional SNS channels. Because NaN transcript is present in SNS-null DRG (Fig. 3) and is expressed preferentially in small sensory neurons (Dib-Hajj et al., 1998), we suggest that the LVA TTX-R persistent current that we describe here is produced by channels encoded by NaN. Although the molecular identity of the channel that produces the LVA TTX-R persistent current cannot be definitively established at this time, the hypothesis that NaN underlies the LVA TTX-R current in small DRG neurons is supported by data showing that the loss of persistent currents in rat small DRG neurons after axotomy (Cummins and Waxman, 1997) is accompanied by a decrease in NaN mRNA levels (Dib-Hajj et al., 1998; Tate et al., 1998).

Patch-clamp studies on HEK293T cells transfected with recombinant NaN (also referred to as SNS2) channels demonstrated a TTX-R sodium current with considerably faster kinetics ($\tau_{inactivation}$ = 1.3 msec at approximately −20 mV) and a greater TTX sensitivity (K_i, ~1 μM) than SNS (Tate et al., 1998). This is surprising because sodium currents with a TTX K_i of 1–2 μM have never been described in DRG neurons. Both SNS and NaN have a serine in the position (S356 in SNS and S355 in NaN) that has been shown (Chen et al., 1992; Satin et al., 1992) to be crucial for TTX resistance, and thus these two channels would be expected to have similar K_i values for TTX. Sivilotti et al. (1997) have demonstrated that mutation of SNS S356 to phenylalanine changes the TTX K_i to 8 nM, suggesting that this serine residue alone confers the high TTX resistance of SNS channels. Therefore, the high TTX resistance of the LVA persistent current in SNS-null neurons is consistent with a channel isoform that has a serine at the TTX binding site.

The difference between the currents recorded in SNS-null DRG neurons (this paper) and the HEK293T current ascribed to NaN by Tate et al. (1998) raises several possibilities. (1) NaN could be differentially processed or modulated in DRG and HEK293T cells. Skeletal muscle sodium (SkM1) channels expressed in *Xenopus* oocytes can have different kinetic properties from native SkM1 channels (Trimmer et al., 1989), and thus differences between HEK293T cells and DRG neurons might account for kinetic differences. However, SkM1, cardiac, and neuronal sodium channels (including SNS) have essentially the same TTX resistance in heterologous expression systems and native cells (Trimmer et al., 1989; Chen et al., 1992; Akopian et al., 1996). Therefore, it seems unlikely that NaN will have a different TTX resistance in DRG neurons and HEK293 cells. (2) NaN might not underlie the LVA persistent TTX-R current that is recorded in SNS-null and WT DRG neurons. If this were the case, it would be expected that TTX-R currents such as those described by Tate et al. (1998) should also be observed in the majority of small DRG neurons of SNS-null mice, because NaN transcript and protein are observed in the majority of small DRG

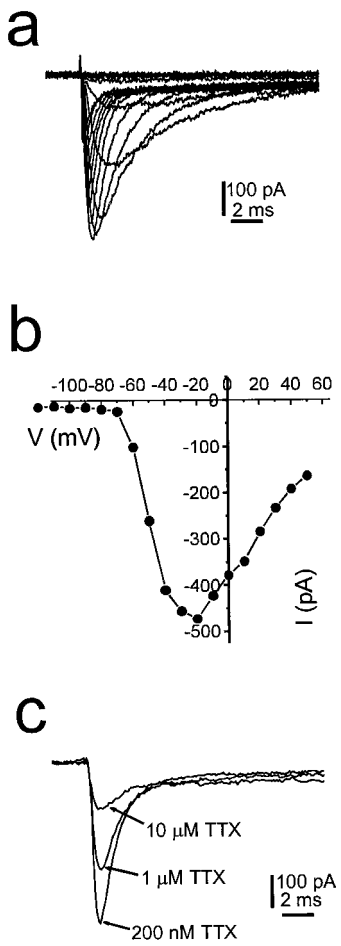

Figure 4. Nontransfected HEK293 cells exhibit an endogenous TTX-R current. *a*, Representative TTX-R currents recorded from a nontransfected HEK293 cell (cell capacitance, 24 pF; access resistance, 1.1 MΩ). A single-exponential decay function fitted to the inactivation phase of the peak current estimated that $\tau_{inactivation}$ = 1.2 msec. The bath solution contained 200 nM TTX. *b*, Peak current–voltage relationship for the currents shown in *a*. The midpoint of activation was −42.4 ± 3.2 mV, and the midpoint of steady-state inactivation was −88.4 ± 1.9 mV for the endogenous TTX-R current in HEK293 cells (n = 4). Recordings were made 3–6 min after establishing the whole-cell configuration. *c*, The endogenous TTX-R current in HEK293 cells is inhibited by TTX with a K_i of 1–2 μM.

neurons (Dib-Hajj et al., 1998; Tate et al., 1998). However, currents like those described by Tate et al. (1998) are not observed in SNS-null neurons. (3) The small current recorded in NaN-transfected HEK293T cells (Tate et al., 1998) might not be encoded by NaN but could be an endogenous TTX-R current that was observed in NaN-transfected HEK293T cells. This possibility is supported by recordings showing small endogenous sodium currents in nontransfected HEK293 cells with the same properties as those ascribed to NaN channels by Tate et al. (Fig. 4). We observed small TTX-R currents in four of five nontransfected HEK293 cells when V_{hold} = −120 mV (peak amplitude = 505 ± 111 pA; n = 4). The properties of these endogenous HEK293 TTX-R currents are strikingly similar to those of cloned cardiac sodium channels (Chahine et al., 1996). Because currents with the properties described by Tate et al. (1998) for NaN are not present in SNS-null neurons but are present in nontransfected HEK293 cells, it is likely that the currents reported by Tate et al. (1998) are endogenous HEK293 currents.

Our observations show that: (1) a distinct TTX-R sodium current is expressed at high densities in small DRG neurons from SNS-null mice; (2) this current has a hyperpolarized voltage dependence compared with SNS; (3) this current is persistent at negative potentials close to resting potential; and (4) this current is present in the majority of small WT DRG neurons. These results provide strong evidence for the presence of a distinct TTX-R sodium channel in addition to SNS, which produces this persistent current in small DRG neurons. Irrespective of the identity of the channel that produces it, it is likely that the low-threshold, persistent TTX-R sodium current that we have identified in SNS-null and WT neurons contributes to subthreshold electrogenesis in C-type primary sensory neurons and affects the excitability of these neurons.

REFERENCES

Akopian AN, Sivilotti L, Wood JN (1996) A tetrodotoxin-resistant voltage-gated sodium channel expressed by sensory neurons. Nature 379:257–262.

Akopian AN, Souslova V, England S, Okuse K, Ogata N, Ure J, Smith A, Kerr BJ, McMahon SB, Boyce S, Hill R, Stanfa LC, Dickenson AH, Wood JN (1999) The tetrodotoxin-resistant sodium channel SNS has a specialized function in pain pathways. Nat Neurosci 2:541–548.

Baker MD, Bostock H (1997) Low-threshold, persistent sodium current in rat large dorsal root ganglion neurons in culture. Neurophysiology 77:1503–1513.

Black JA, Dib-Hajj S, McNabola K, Jeste S, Rizzo MA, Kocsis JD, Waxman SG (1996) Spinal sensory neurons express multiple sodium channel a-subunit mRNAs. Mol Brain Res 43:117–132.

Black JA, Dib-Hajj S, Cohen S, Hinson AW, Waxman SG (1998) Glial cells have heart: rH1 Na+ channel mRNA and protein in spinal cord astrocytes. Glia 23:200–208.

Chahine M, Deschene I, Chen LQ, Kallen RG (1996) Electrophysiological characteristics of cloned skeletal and cardiac muscle sodium channels. Am J Physiol 271:H498–H506.

Chen LQ, Chahine M, Kallen RG, Barchi RL, Horn R (1992) Chimeric study of sodium channels from rat skeletal and cardiac muscle. FEBS Lett 309:253–257.

Crill WE (1996) Persistent sodium currents in mammalian central neurons. Annu Rev Physiol 58:349–362.

Cummins TR, Waxman SG (1997) Down-regulation of TTX-resistant sodium currents and upregulation of a rapidly repriming TTX-sensitive sodium current in small spinal sensory neurons after nerve injury. J Neurosci 17:3503–3514.

Dib-Hajj SD, Tyrrell L, Black JA, Waxman SG (1998) NaN, a novel voltage-gated Na channel, is expressed preferentially in peripheral sensory neurons and down-regulated after axotomy. Proc Natl Acad Sci USA 95:8963–8968.

Dib-Hajj SD, Tyrrell L, Escayg A, Wood, PM, Meisler MH, Waxman SG (1999) Coding sequence, genomic organization and conserved chromosomal localization of the mouse gene Scn11a encoding the sodium channel NaN. Genomics 59:309–318.

Donahue LM (1995) The tetrodotoxin-insensitive sodium current in rat dorsal root ganglia is unlikely to involve the expression of the tetrodotoxin-resistant sodium channel, SkM2. Neurochem Res 20:713–717.

Kapoor R, Li YG, Smith KJ (1997) Slow sodium-dependent potential oscillations contribute to ectopic firing in mammalian demyelinated axons. Brain 120:647–652.

Kostyuk PG, Veselovsky NS, Tsyndrenko AY (1981) Ionic currents in the somatic membrane of rat dorsal root ganglion neurons—I. Sodium currents. Neuroscience 6:2423–2430.

Parri HR, Crunelli V (1998) Sodium current in rat and cat thalamocortical neurons: role of a non-inactivating component in tonic and burst firing. J Neurosci 18:854–867.

Rizzo MA, Kocsis JD, Waxman SG (1994) Slow sodium conductances of dorsal root ganglion neurons: intraneuronal homogeneity and interneuronal heterogeneity. J Neurophysiol 72:2796–2815.

Rush AM, Brau ME, Elliott AA, Elliott JR (1998) Electrophysiological properties of sodium current subtypes in small cells from adult rat dorsal root ganglia. J Physiol (Lond) 511:771–789.

Sangameswaran L, Delgado SG, Fish LM, Koch BD, Jakeman LB, Stewart GR, Sze P, Hunter JC, Eglen RM, Herman RC (1996) Structure and function of a novel voltage-gated tetrodotoxin-resistant sodium channel specific to sensory neurons. J Biol Chem 271:5953–5956.

Satin J, Kyle JW, Chen M, Bell P, Cribbs LL, Fozzard HA, Rogart RB (1992) A mutant of TTX-resistant cardiac sodium channels with TTX-sensitive properties. Science 256:1202–1205.

Scholz A, Appel N, Vogel W (1998) Two types of TTX-resistant and one TTX-sensitive Na+ channel in rat dorsal root ganglion neurons and their blockade by halothane. Eur J Neurosci 10:2547–2556.

Schwindt PC, Crill WE (1995) Amplification of synaptic current by persistent sodium conductance in apical dendrite of neocortical neurons. J Neurophysiol 74:2220–2224.

Sivilotti L, Okuse K, Akopian AN, Moss S, Wood JN (1997) A single serine residue confers tetrodotoxin insensitivity on the rat sensory-neuron-specific sodium channel SNS. FEBS Lett 409:49–52.

Stafstrom CE, Schwindt PC, Crill WE (1982) Negative slope conductance due to a persistent subthreshold sodium current in cat neocortical neurons in vitro. Brain Res 236:221–226.

Tate S, Benn S, Hick C, Trezise D, John V, Mannion RJ, Costigan M, Plumpton C, Grose D, Gladwell Z, Kendall G, Dale K, Bountra C, Woolf CJ (1998) Two sodium channels contribute to the TTX-R sodium current in primary sensory neurons. Nat Neurosci 1:653–555.

Trimmer JS, Cooperman SS, Tomiko SA, Zhou JY, Crean SM, Boyle MB, Kallen RG, Sheng ZH, Barchi RL, Sigworth FJ, Goodman RH, Agnew WS, Mandel G (1989) Primary structure and functional expression of a mammalian skeletal muscle sodium channel. Neuron 3:33–49.